SATURATION COMPENSATION SCHEMES FOR VECTOR CONTROLLED INDUCTION MOTOR DRIVES

Emil Levi
Dept. of El.Engineering
University of Novi Sad
Novi Sad, Yugoslavia

Slobodan Vukosavić
El. Eng. Institute
"Nikola Tesla"
Belgrade, Yugoslavia

Vladan Vučković
Dept. of El.Engineering
University of Belgrade
Belgrade, Yugoslavia

ABSTRACT

The schemes used in field-oriented induction machines for rotor flux estimation and indirect vector control are derived from constant parameter induction machine model. However, the parameters of the machine are subject to variation due to temperature changes and variable degree of saturation. As a consequence, detuned operation of the drive results. The paper deals with modifications that are necessary in the structures of rotor flux computers and indirect vector controller in order to take into account main flux saturation. The discussed schemes are based on measurement of main flux and stator currents, stator voltages and stator currents and stator currents and rotor speed. Verification of the proposed saturated rotor flux calculators and indirect vector controllers is provided by the aid of digital simulation. One of the schemes is applied in a vector controlled induction motor drive and experimental results are included.

1. INTRODUCTION

The schemes that are usually used in vector controlled induction machines for rotor flux estimation are derived from constant parameter induction machine models. The same is valid for indirect (feedforward) type of vector control. Unfortunately, the machine parameters are subject to variation due to temperature changes and saturation. As a consequence, mismatch between actual parameters and parameters used in the control part of the system occurs, leading to detuned operation of the drive. Depending on the applied vector control structure, performance can be influenced by stator or rotor resistance variation, leakage inductance and magnetizing inductance variation.

The influence of rotor resistance variation on performance of a field-oriented induction machine is investigated in [1-4] and numerous means for compensation are proposed in [4-8]. The influence of variable degree of saturation on steady-state operation of the drive is treated in [1,2,9,10] while the proper selection of flux level under saturated conditions is elaborated in [11]. A method for on-line estimation of mutual inductance in steady-state operation is proposed in [12]. The saturated dynamic models of induction machines with field-oriented control are discussed in [13-15], where it is shown that the equations which describe current-fed induction machine under saturated conditions are not decoupled as they are if the saturation effect is absent or neglected.

The rate of change of saturation level is determined with the rate of change of currents and it can be very rapid in high performance drives, as shown in [15]. Therefore, it is not possible to compensate for saturation influence during transients with schemes which are usually applied for rotor time constant adaptation, due to certain amount of time which is needed for signal acquisition, processing and execution of identification algorithm. Some reduction of sensitivity to saturation effect and other parameter variations is possible if the observers are applied [16-18], however the estimation error in rotor flux due to saturation effect cannot be eliminated in this way. Considerations given above lead to the conclusion that certain improvement is necessary in induction machine models that constitute basis for vector control, if the saturation influence is to be compensated.

The paper presents modified structures of rotor flux computers and indirect vector controller, that are derived in such a way that nonlinear relationship between main flux and magnetizing current is taken into account. Discussed rotor flux computers are common types, based on main flux and stator currents (ψ_m-i_s estimator), stator voltages and stator currents (u_s-i_s scheme), and stator currents and rotor speed or position (i_s-ω calculator) as measured variables, respectively. The emphasis is placed on simplified saturated versions of indirect vector controller and rotor flux estimator of the i_s-ω type. These schemes can be used in practical realizations without difficulties, and they still provide satisfactory operation of the drive with respect to main flux saturation. Stator and rotor resistances and leakage inductances are treated as constant parameters. The developed schemes are verified by the aid of digital simulation. One of the structures is tested and experimental results are included.

The paper is organized as follows. The second section at first gives description and mathematical representation of the drive for simulation purposes. The modified schemes aimed for rotor flux computation under saturated conditions are then presented. The third section is devoted to

CH2873-8/90/0000-0591 $1.00

structural changes which are needed in indirect type of vector control in order to take into account saturation effect. The fourth section displays simulation results and, finally, the fifth section contains a sample of experimental results.

2. ROTOR FLUX COMPUTATION UNDER SATURATED CONDITIONS

The simplified representation of a vector controlled induction machine is given in Fig. 1. The machine is assumed to be current fed from a current regulated PWM inverter (block CRPWM in Fig. 1).

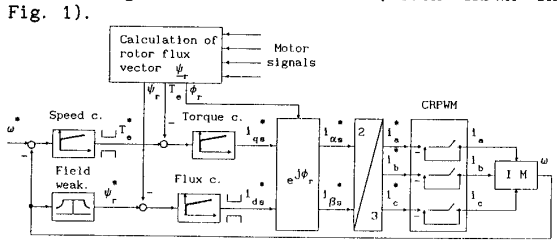

Fig. 1 - Current-fed vector controlled induction motor

For simulation purposes block CRPWM is substituted with first order delay, having a time constant of $T_1 = 0,5ms$. This value is sufficiently small to enable omission of the decoupling circuit for inverter lag compensation in the control part of the drive [19]. The data of induction machine employed in digital simulation are given in Appendix, together with its magnetizing curve obtained from no-load test. Controllers are of the PI type. Rate-of-change limiter is applied for the speed command. Maximum allowed values of torque command and stator d-axis current command are limited.

The induction machine is represented with saturated current state space model [20,21] in the stationary reference frame. Due to assumed current feeding stator equations are omitted and stator axis currents and their derivatives act as input variables into induction machine model. The model is given in detail in [22].

The structure of the flux estimator depends on available motor signals. The modifications of basic flux computer structures that enable accurate estimation with respect to saturation effect are discussed below.

2.1. Saturated $\psi_m - i_s$ calculator

After three to two phase transformation is performed, stator current and main flux components are the inputs in the flux computer that operates in stationary α,β reference frame. Computation is based on the following equations

$$\psi_m = \sqrt{\psi_{\alpha m}^2 + \psi_{\beta m}^2} \qquad i_m = f(\psi_m)$$

$$i_{\alpha m} = \frac{\psi_{\alpha m}}{\psi_m} i_m \qquad i_{\beta m} = \frac{\psi_{\beta m}}{\psi_m} i_m \tag{1}$$

$$i_{\alpha m} = i_{\alpha s} + i_{\alpha r} \qquad i_{\beta m} = i_{\beta s} + i_{\beta r}$$

$$\psi_{\alpha r} = \psi_{\alpha m} + L_{\gamma r}\left[i_{\alpha m}(\psi_m) - i_{\alpha s}\right] \tag{2}$$

$$\psi_{\beta r} = \psi_{\beta m} + L_{\gamma r}\left[i_{\beta m}(\psi_m) - i_{\beta s}\right]$$

$$\psi_r = \sqrt{\psi_{\alpha r}^2 + \psi_{\beta r}^2} \tag{3}$$

$$\cos\varphi_r = \psi_{\alpha r}/\psi_r \qquad \sin\varphi_r = \psi_{\beta r}/\psi_r$$

$$T_e = \frac{3}{2} P\,(\psi_{\alpha m} i_{\beta s} - \psi_{\beta m} i_{\alpha s}) \tag{4}$$

The nonlinear relationship $i_m = f(\psi_m)$ in Eq. (1) represents inverse of the induction machine magnetizing curve. Calculation of machine torque can alternatively be done by the aid of

$$T_e = \frac{3}{2} P\,(\psi_{\alpha r}\,\psi_{\beta m} - \psi_{\beta r}\,\psi_{\alpha m})/L_{\gamma r} \tag{4a}$$

Saturated flux computer based on Eqns. (1)-(3),(4a) is shown in Fig. 2. It should be noted that this scheme has already been presented in [15]. It is included here only for the sake of completeness. The angle φ_m in Fig. 2 denotes instantaneous angular position of main flux space vector with respect to the stationary reference frame.

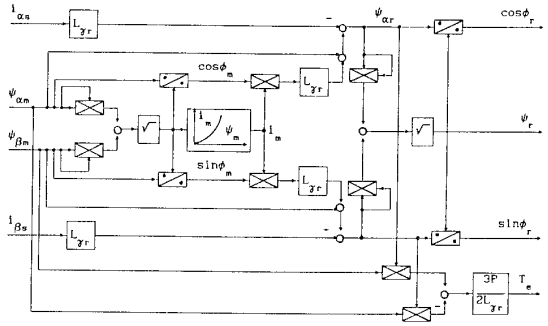

Fig. 2 - Saturated $\psi_m - i_s$ flux computer

2.2. Saturated $u_s - i_s$ computer

If the stator voltages and currents are measured, saturated flux estimator can be described with the following equations in the stationary reference frame

$$\psi_{\alpha s} = \int (u_{\alpha s} - R_s i_{\alpha s})dt \qquad \psi_{\beta s} = \int (u_{\beta s} - R_s i_{\beta s})dt \tag{5}$$

$$\psi_{\alpha m} = \psi_{\alpha s} - L_{\gamma s} i_{\alpha s} \qquad \psi_{\beta m} = \psi_{\beta s} - L_{\gamma s} i_{\beta s} \tag{6}$$

$$\psi_m = \sqrt{\psi_{\alpha m}^2 + \psi_{\beta m}^2} \qquad i_m = f(\psi_m)$$

$$i_{\alpha m} = \frac{\psi_{\alpha m}}{\psi_m} i_m \qquad i_{\beta m} = \frac{\psi_{\beta m}}{\psi_m} i_m \tag{7}$$

$$\psi_{\alpha r} = \psi_{\alpha m} + L_{\gamma r}\left[i_{\alpha m}(\psi_m) - i_{\alpha s}\right]$$

$$\psi_{\beta r} = \psi_{\beta m} + L_{\gamma r}\left[i_{\beta m}(\psi_m) - i_{\beta s}\right] \tag{8}$$

$$\psi_r = \sqrt{\psi_{\alpha r}^2 + \psi_{\beta r}^2} \tag{9}$$

$$\cos\varphi_r = \psi_{\alpha r}/\psi_r \qquad \sin\varphi_r = \psi_{\beta r}/\psi_r$$

$$T_e = \frac{3}{2} P (\psi_{\alpha s} i_{\beta s} - \psi_{\beta s} i_{\alpha s}) \quad (10)$$

The computer is depicted in Fig. 3.

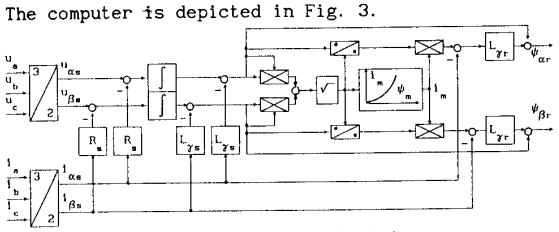

Fig. 3 - The saturated u_s-i_s calculator

Direct comparison of the saturated ψ_m-i_s and u_s-i_s schemes shows that they are identical with respect to saturation effect. In the ψ_m-i_s scheme measured values of $\psi_{\alpha m}, \psi_{\beta m}$ are saturated values, no matter whether saturation effect is incorporated in the model or not, and the torque value obtained by the aid of Eq. (4) is correct value regarding saturation. The calculated values of $\psi_{\alpha s}, \psi_{\beta s}$ and $\psi_{\alpha m}, \psi_{\beta m}$ in u_s-i_s scheme are saturated values as well and the value of torque, Eq. (10), always corresponds to actual saturation degree. Therefore these two schemes can be in error only in rotor flux amplitude and position estimation, if the saturation effect is not taken into account in Eqns. (2)-(3) and Eqns. (8)-(9), respectively, that are the same for the both schemes. Detailed treatment of saturated u_s-i_s estimator is given in [23].

2.3. Saturated i_s-ω computer

The estimation of rotor flux amplitude and position on the basis of stator currents and rotor speed measurement is usually performed in rotor flux oriented d,q reference frame. Saturated rotor flux computer is then given with

$$T_\lambda \, d\psi_r/dt + \psi_r = \psi_{dm} \quad (11)$$

$$\omega_r - \omega = \psi_{qm}/(T_\lambda \psi_r)$$

$$\psi_{dm} = \psi_r + L_{\gamma r}\left[i_{ds} - i_{dm}(\psi_m)\right] \quad (12)$$

$$\psi_{qm} = L_{\gamma r}\left[i_{qs} - i_{qm}(\psi_m)\right]$$

$$T_e = \frac{3}{2} P \psi_r \psi_{qm}/L_{\gamma r} \quad (13)$$

$$d\varphi_r/dt = \omega_r \quad (14)$$

where Eqns. (1) remain valid with appropriate change of indices, $\alpha \to d$, $\beta \to q$, and $\psi_r = \psi_{dr}$. The saturated calculator is shown in Fig. 4. The time constant T_λ is defined as $T_\lambda = L_{\gamma r}/R_r$.

2.4. Simplified saturated i_s-ω calculator

When the calculation is done in rotational d-q reference frame, simplification is possible. Taking into account that, if the field-orientation is maintained, the condition $\psi_{qr} = 0$ is satisfied,

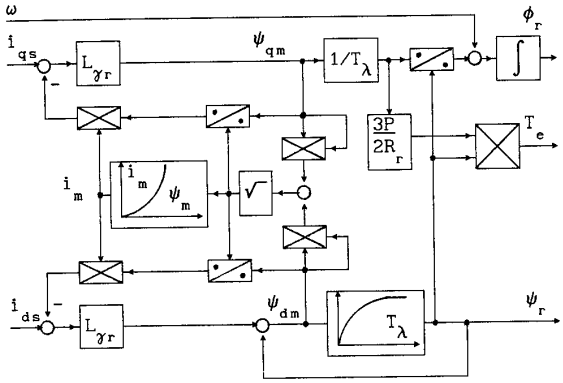

Fig. 4 - Saturated i_s-ω calculator in rotor flux oriented reference frame

the influence of q-axis magnetizing flux $\psi_{qm} = -L_{\gamma r} i_{qr} = L_{\gamma r} (L_m/L_r) i_{qs}$ on resultant magnetizing flux can be neglected. This assumption proves to be satisfactory for the drives which operate with low adjusted torque limit of the order three times rated or less, as shown in [22]. The approximate saturated flux computer is then described with Eqns. (15)-(17) and is shown in Fig. 5.

$$T_\lambda \, d\psi_r/dt + \psi_r = \psi_{dm} \quad (15)$$

$$\omega_r - \omega = \frac{L_m}{L_r} R_r i_{qs}/\psi_r$$

$$\psi_{dm} = \psi_r + L_{\gamma r}\left[i_{ds} - i_{dm}(\psi_m)\right] \quad (16)$$

$$T_e = \frac{3}{2} P \frac{L_m}{L_r} i_{qs} \psi_r \quad (17)$$

The approximation $\psi_m \approx \psi_{dm}$, $i_m \approx i_{dm}$ is taken into account and $L_m = \psi_{dm}/i_{dm}$, $L_r = L_m + L_{\gamma r}$. Eq. (14) determines the angular position of the rotor flux space vector.

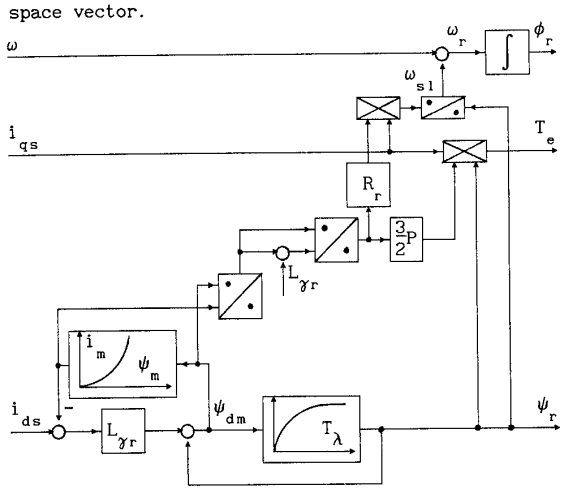

Fig. 5 - Simplified saturated i_s-ω calculator in rotational reference frame

It is to be noted that slip frequency and torque estimation are dependent on the ratio L_m/L_r. The change of L_m/L_r ratio with change of saturation level is very small and as a further simplification it can be neglected as well. The calculator equations become ($\psi_m \approx \psi_{dm}$, $i_m \approx i_{dm}$)

$$T_\lambda \, d\psi_r/dt + \psi_r = \psi_{dm} \qquad (18)$$

$$\omega_r - \omega = K_1 \, i_{qs}/\psi_r \qquad K_1 = L_m/T_r = \text{const}$$

$$\psi_{dm} = \psi_r + L_{\gamma r}\left[i_{ds} - i_{dm}(\psi_m)\right] \qquad (19)$$

$$T_e = K_2 i_{qs} \psi_r \qquad K_2 = \frac{3}{2} P \, L_m/L_r = \text{const} \qquad (20)$$

The scheme is given in Fig.6.

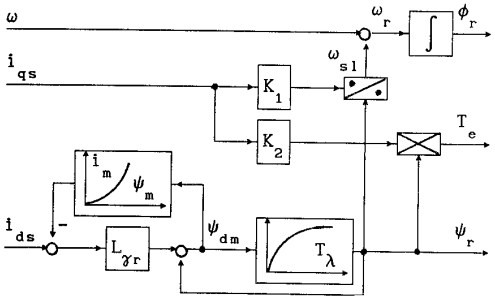

Fig. 6 - The simplest form of saturated i_s-ω computer

3. SATURATED INDIRECT VECTOR CONTROLLER

Conventional indirect vector controller is based on the same induction machine model, as is the unsaturated rotor flux estimator of the i_s-ω type. It is shown in Fig. 7. Therefore, it is possible to construct saturated indirect vector controller following the same approach that was

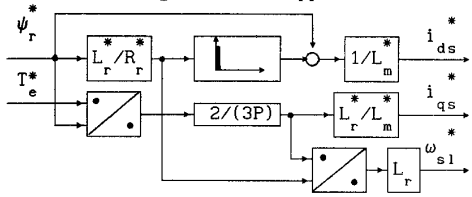

Fig. 7 - Unsaturated indirect vector controller

used in the previous section for development of the saturated i_s-ω calculator. Taking into account that the main reason why indirect vector control is so widespread, is its simple structure, it seems inappropriate to discuss a controller that would correspond to Eqns. (11)-(14), Fig. 4, and that fully accounts for main flux saturation. Simplified saturated indirect vector controller can be obtained on the basis of Eqns. (14)-(17). It is shown in Fig. 8 and described with the following equations

$$\psi_m \approx \psi_{dm} = T_\lambda d\psi_r^*/dt + \psi_r^* \qquad (21)$$

$$i_{ds}^* = i_{dm}(\psi_m) + (1/L_{\gamma r}) T_\lambda d\psi_r^*/dt \qquad (22)$$

$$\omega_{sl}^* = (2/3P) R_r T_e^*/(\psi_r^*)^2 \qquad \phi_r = \int (\omega_{sl}^* + \omega)dt \qquad (23)$$

$$i_{qs}^* = (2/3P)\,(L_{\gamma r} + L_m)/L_m \; T_e^*/\psi_r^* \qquad (24)$$

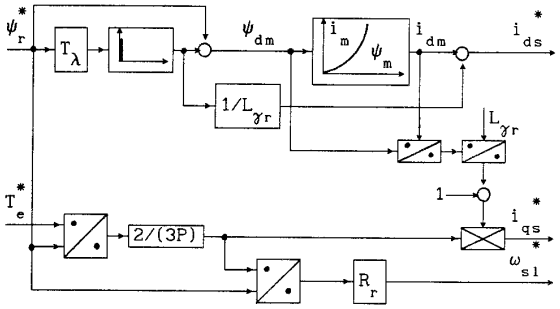

Fig. 8 - Simplified saturated indirect vector controller

If, as a further simplification, the change of L_m/L_r ratio is neglected, the simplest form of saturated indirect vector controller results, Fig.9. The scheme is described with Eqns. (21)-(22) and with Eqns. (25)-(26)

$$\omega_{sl}^* = K_1 i_{qs}^*/\psi_r^* \qquad K_1 = L_m^*/T_r^* = \text{const} \qquad (25)$$

$$i_{qs}^* = (1/K_2)\, T_e^*/\psi_r^* \qquad K_2 = (3/2) P L_m^*/L_r^* = \text{const} \qquad (26)$$

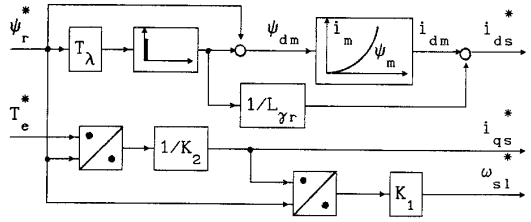

Fig. 9 - The simplest saturated indirect vector controller

Detailed study of main flux saturation influence on the behaviour of a field-oriented induction machine with indirect vector control is presented in [24]. The simulation results given in the next section, that apply to indirect vector control, are aimed for verification of the accuracy of the schemes given in Figs. 8 and 9. For simulation purposes, induction machine is represented with saturated flux state-space model in the rotational reference frame determined with the angle ϕ_r, calculated by the indirect vector controller. The model is given in [24]. Ideal current control is assumed in this case.

4. SIMULATION RESULTS

A sample of simulation results is given here. Fig. 10 illustrates operation of the drive with saturated i_s-ω computer in rotor flux oriented reference frame, that provides all the necessary information for control purposes. Previous steady-state corresponds to operation with rated rotor flux, two thirds of the rated speed and load torque equal to one half of the rated torque. At

first, acceleration to full speed is commanded. Later on, speed demand is increased to four thirds of the rated speed and field-weakening region is entered. Fig. 10 shows that the saturated i_s-ω computer can provide accurate information about the actual value of rotor flux, no matter whether the saturation level is changed due to q-axis component of the magnetizing current (rapid acceleration in the constant flux region with high value of maximum allowed torque) or due to change in d-axis magnetizing current component (operation in the field-weakening region). Superscript "e" denotes outputs of the flux computer.

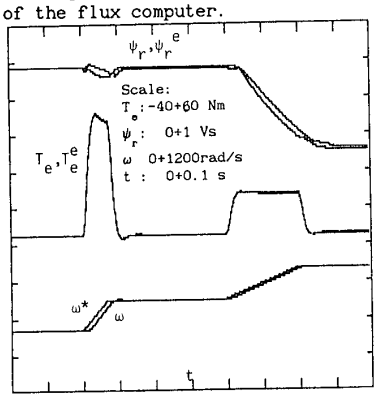

Fig. 10 - Acceleration in the constant flux region and operation in the field-weakening region with saturated i_s-ω computer in rotational reference frame

Operation in the field-weakening region, with the simplest saturated i_s-ω computer, described with Eqns. (18)-(20), is shown in Fig. 11. Previous steady-state corresponds to operation with rated rotor flux, 80% of the rated speed and rated load torque. Speed command is changed to 120% of the rated speed and later on is brought back to its initial value. The calculator neglects q-axis magnetizing flux influence on resultant main flux and therefore it cannot provide accurate estimation during acceleration where q-axis magnetizing flux attains relatively high value (maximum value of torque during acceleration is about four times rated). However, it accounts for change in saturation level caused by operation with reduced flux and provides accurate estimates during operation in the field-weakening region. For comparison purposes, Fig. 11 contains corresponding responses obtained with the unsaturated rotor flux calculator, with the magnetizing inductance set to constant rated value.

It should be noted that the response obtained with simplified saturated i_s-ω computer, Fig. 5, is practically identical to the one shown in Fig. 11a. Therefore, it is not included here.

In order to verify developed saturated structures of indirect vector controllers the following approach is utilized. It is assumed that the drive operates in the torque mode (i.e., with speed loop open), the torque command is initially zero and the machine is excited by the aid of unsaturated indirect vector controller to a certain level of rotor flux. At the instant t_1 the control

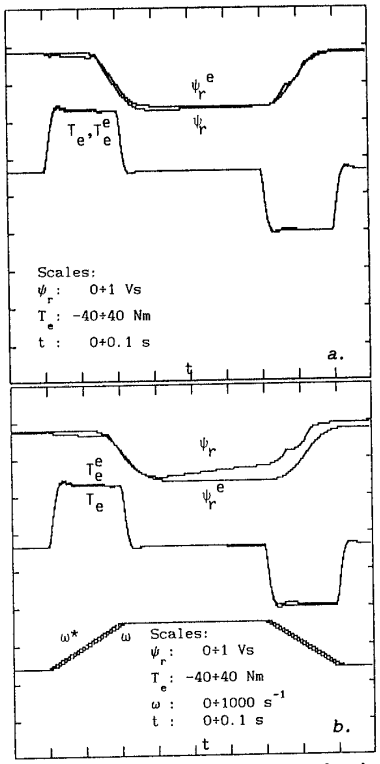

Fig. 11 - Operation in the field-weakening region with the simplest i_s-ω computer (a.) and with unsaturated flux computer (b.)

scheme is switched from unsaturated to the appropriate saturated vector controller, and at instant t_2 torque command is applied. Fig. 12 shows results for the application of the simplified saturated and the simplest saturated indirect vector controllers. The operating conditions are $\psi_r^* = \psi_{rn}/1.33$, $T_e^* = T_{en}$ and the value of the magnetizing inductance in unsaturated scheme that is active till the instant t_1 is equal to rated.

Due to initial application of unsaturated controller there is a mismatch between commanded and actual value of rotor flux. Application of the both saturated versions provides convergence of actual to commanded value of rotor flux. The torque response is slightly poorer with the simplest saturated structure due to approximation L_m/L_r = const. (the value of L_m is set equal to rated).

Finally, Fig. 13 illustrates operation in the constant flux region, with initially erroneously set value of magnetizing inductance in the unsaturated scheme, $L_m^* = 1.45L_{mn}$. The simulation procedure is the same as in Fig. 12, except that $\psi_r^* = \psi_{rn}$ and $T_e^* = 3T_{en}$. The both saturated versions again provide convergence of actual to commanded rotor flux. Due to application of rather high

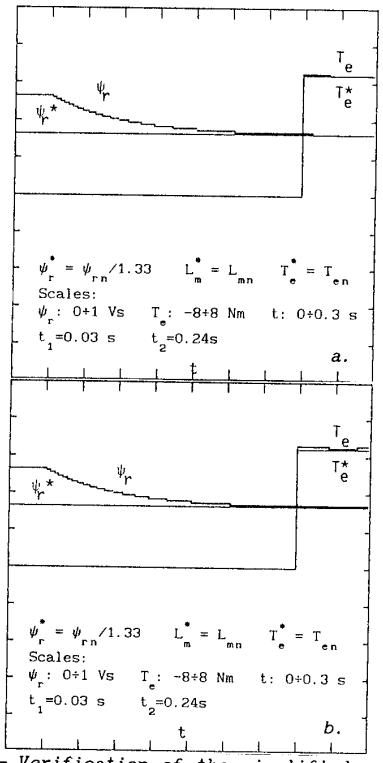

Fig. 12 - Verification of the simplified saturated (a.) and the simplest saturated (b.) indirect vector controllers for operation with reduced level of rotor flux

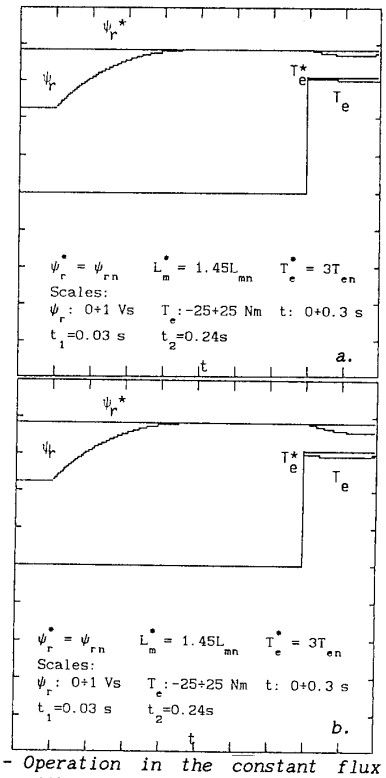

Fig. 13 - Operation in the constant flux region with simplified saturated (a.) and the simplest saturated indirect vector controller

torque command, the existence of q-axis magnetizing current that is neglected in the controllers causes certain discrepancy between actual and commanded torque, as well as a small reduction in rotor flux amplitude. The differences are again more pronounced in the case of the simplest saturated controller application due to assumption L_m/L_r = const, where L_m is taken inadequately high, equal to $1.45L_{mn}$.

The presented simulation results show that the developed saturated rotor flux computers are capable of providing accurate estimates of rotor flux amplitude and position and thus they enable compensation for saturation influence in field-oriented induction motor drives.

5. EXPERIMENTAL VERIFICATION

The simplified saturated indirect vector controller shown in Fig. 8 was applied in experimental study. The response to sudden loading and unloading of the machine with 85% of the rated torque is shown in Fig. 14. The applied stator d-axis current command is 70% of the rated value. Fig. 14a is valid for simplified saturated controller application while Fig. 14b corresponds to application of unsaturated controller. Direct comparison of the responses shows that there are hardly any differences between them, although the simplified saturated controller sets the rotor time constant to correct value, $T_r^* = 1,215T_{rn}$, while the unsaturated controller operates with rated value of rotor time constant. This is an expected result, because speed control loop suppresses the effects of parameter deviation effectively, [1]. However, the principal difference between responses shown in Fig. 14 lies in the fact that the level of applied stator d-axis current command corresponds to significantly different levels of rotor flux commands. If the saturated scheme is applied, the commanded rotor flux equal to 82% of the rated leads to stator d-axis current command equal to 70% of the rated value. In the case of unsaturated scheme application the stator d-axis current command equal to 70% of the rated corresponds to rotor flux command equal to 70% of the rated value.

Finally, an optimal efficiency vector controlled induction motor drive is realized. In this case the level of rotor flux has to be varied in accordance with load torque. Under light load, operation with reduced flux leads to maximum efficiency. The value of stator d-axis current command has to be set in such a way that it corresponds to rotor flux that gives optimal efficiency for the given load. Therefore magnetizing curve of the machine should be incorporated in the controller. The structure employed in realization is the one shown in Fig. 9. The detailed description of the drive is given in [25]. The data of the machine used in experimental

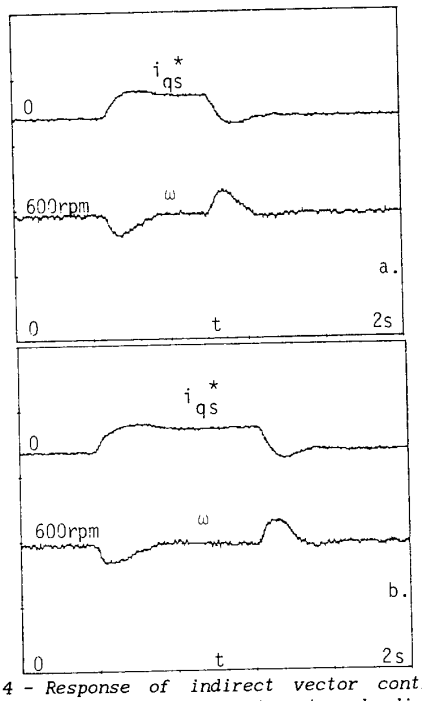

Fig. 14 - Response of indirect vector controlled induction machine to step loading and unloading in the reduced flux region
a. with saturated simplified controller
b. with unsaturated controller

investigation are given in Appendix. Fig. 15 shows experimentally obtained traces of the flux in the controller and induction motor speed. The previous steady state corresponds to operation with zero load torque and 20% of the rated flux. Load torque equal to two times rated is applied.

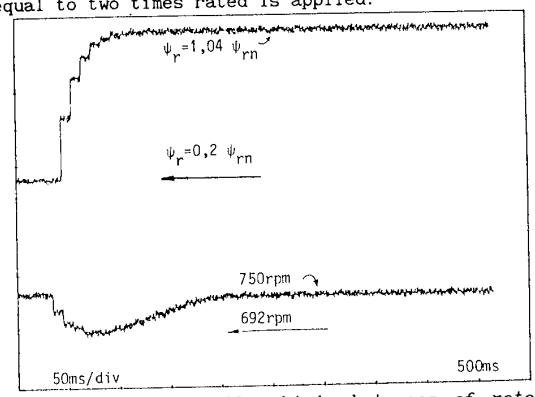

Fig. 15 - Experimentally obtained traces of rotor flux (upper trace) and machine speed (lower trace) in an optimal efficiency vector controlled drive, with saturation taken into account in the controller

6. CONCLUSION

The paper describes a number of rotor flux computer structures which take into account main flux saturation and therefore are capable of providing correct estimates of torque and rotor flux amplitude and position irrespective of the actual degree of saturation in the machine. The schemes discussed are based on measurement of main flux and stator currents, stator voltages and currents, and stator currents and rotor speed, respectively. Saturated indirect vector controllers are elaborated as well. The attention is focused mainly towards calculator based on stator currents and rotor speed as measured variables, where full order computers and simplified versions are given, and towards simplified saturated indirect vector controllers. Verification of the schemes is done by the aid of digital simulation. One of the schemes is incorporated in a vector controlled induction motor drive and a sample of experimental results is included.

7. REFERENCES

1. K.B.Nordin, D.W.Novotny, D.S.Zinger; The influence of motor parameter deviations in feedforward field-oriented drive systems, *IEEE Trans. on Industry Applications,* Vol. IA-21, No.4, pp. 1009-1115, 1985.
2. R.Krishnan, P.Pillay; Parameter sensitivity in vector controlled AC motor drives, *IEEE IES Annual Meeting IECON,* Cambridge MA, pp. 212-218, 1987.
3. S.Bolognani, G.S.Buja; Parameter variation and computation error effects in indirect field-oriented induction motor drives, *Proc. of the ICEM '88,* Pisa (Italy), Part III, pp. 545-549, 1988.
4. L.J.Garces; Parameter adaption for the speed controlled static AC drive with a squirrel-cage induction motor, *IEEE Trans. on Ind. App.,* Vol. IA-16, No.2, pp. 173-178, 1980.
5. F.Loeser, P.K.Sattler; Identification and compensation of the rotor temperature of AC drives by an observer, *IEEE Trans. on Ind. App.,* Vol. IA-21, No.6, pp. 1387-1393, 1985.
6. T.Matsuo, T.A.Lipo; Rotor resistance identification in the field-oriented control of a squirrel cage induction motor, *IEEE Trans. on Ind. App.,* Vol. IA-21, No.3, pp. 624-632, 1985.
7. W.Schumacher, G.Heinemann; Fully digital control of induction motor as servo drive, *Proc.of the EPE'85,* Brussels, pp. 2.191-2.196, 1985.
8. L.C.Zai, T.A.Lipo; An extended Kalman filter approach to rotor time constant measurement in PWM induction motor drives, *IEEE IAS Annual Meeting,* Atlanta, Georgia, pp. 173-183, 1987.
9. R.Krishnan, F.C.Doran; Study of parameter sensitivity in high performance inverter fed induction motor drive systems, *IEEE Trans. on Ind. App.,* Vol. IA-23, No. 4, pp. 623-635, 1987.
10. R.D.Lorenz, D.W.Novotny; Saturation effects in field oriented induction machines, *IEEE IAS Annual Meeting,* Atlanta, Georgia, pp. 150-155, 1987.
11. F.M.H.Khater, R.D.Lorenz, D.W.Novotny, K.Tang; Selection of flux level in field oriented induction machine controllers with consideration of magnetic saturation, *IEEE Trans. on Ind. App.,* Vol. IA-23, No.2, pp. 276-282, 1987.
12. S.K.Sul; A novel technique of rotor resistance estimation considering variation of mutual inductance, *IEEE IAS Annual Meeting,* Atlanta, Georgia, pp. 184-188, 1987.

13. P. Vas, M. Alakula, J. E. Brown, K. E. Hallenius; Field-oriented control of saturated AC machines, *IEEE Conf. on Power Electronics and Variable Speed Drives,* Conf. Pub. No. 291, London, pp. 283-286, 1988.
14. E. Levi, V. Vučković; Field-oriented control of a current-fed saturated induction machine, *Proc. of the Middle East Power System Conf.,* Cairo, pp. 630-635, 1989.
15. E. Levi, V. Vučković; Field-oriented control of induction machines in the presence of magnetic saturation, *Electric Machines and Power Systems,* Vol. 16, No. 2, pp. 133-147, 1989.
16. A. Bellini, G. Figalli, G. Ulivi; A microprocessor based state observer for the feedback control of induction motor drives, *Proc. of the EPE'85,* Brussels, pp. 3.45-3.50, 1985.
17. A. Bellini, G. Figalli, G. Ulivi; A microcomputer based direct field oriented control of induction motors, *Proc. ICEM '86,* Munchen, pp. 652-655, 1986.
18. G. Verghese, S. R. Sanders; Observers for flux estimation in induction machines, *IEEE Trans. on Ind. Electronics,* Vol. IE-35, No. 1, pp. 85-94, 1988.
19. H. Bausch, H. Hontheim, H. D. Kolletshke; The influence of decoupling methods on the dynamic behavior of field-oriented controlled induction machine, *Proc. of the ICEM '86,* Munchen, pp. 648-651, 1986.
20. I. Boldea, S. Nasar; A unified treatment of magnetic saturation in orthogonal axis models of electric machines, *Electric Machines and Power Systems,* Vol. 12, No. 3, pp. 195-204, 1987.
21. J. E. Brown, K. P. Kovacs, P. Vas; A method of including the effects of main flux path saturation in the generalized equations of AC machines, *IEEE Trans. on Power App. and Systems,* Vol. PAS-102, No. 1, pp. 96-103, 1983.
22. V. Vučković, E. Levi; Rotor flux calculator for saturated induction machines with field-oriented control, *3rd European Conf. on Power Electronics and Applications EPE'89,* Aachen (W. Germany), pp. 505-510, 1989.
23. E. Levi, V. Vučković; A method of rotor flux estimation in saturated field-oriented induction machines, *ICEM'90,* Cambridge, MA, August 1990.
24. E. Levi, V. Vučković, S. Vukosavić; Study of main flux saturation effects in field-oriented induction motor drives, *IEEE IES Annual Meeting IECON'89,* Philadelphia, PA, pp. 219-224, 1989.
25. S. Vukosavić; *Design of adaptive microprocessor system for induction motor speed and position control,* Ph. D. Thesis, University of Belgrade, 1989.

8. APPENDIX

Motor data:

0,75 kW 2P = 4 220/380 V 3,6/2,1 A
R_s=10Ω R_r=6,3Ω $L_{\gamma s}$=43,067 mH
$L_{\gamma r}$=40,107 mH L_{mn}=0,42119H J=0,00442 kgm^2
T_{en}=5,15 Nm i_{qsn}/i_{dsn}=1

Main flux and dynamic inductance are given in Fig. A1.

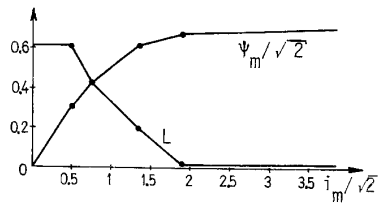

Fig. A1 - Piece-wise linear approximation of dynamic inductance and main flux

Data of the machine used in optimal efficiency drive:
1kW Y/380V 2,8A cosφ=0,78 2P=4 1300rpm